

Supplemental information:

Hoeke RK, Damlamian H, Aucan J and Wandres M (2020) Severe Flooding in the Atoll Nations of Tuvalu and Kiribati Triggered by a Distant Tropical Cyclone Pam. *Front. Mar. Sci.* 7:539646. doi: 10.3389/fmars.2020.539646

Section 1: Assessment of the CAWCR Wave Hindcast wave height during Tropical Cyclone PAM

Numerical models such as the one underpinning the CAWCR wave hindcast used in this study (Durrant et al. 2014; Hemer et al. 2016) are known to sometimes perform poorly when used to simulate wave fields associated with tropical cyclones (TCs). However, recent formulations of “source term” (ST) physics have largely removed overestimation of wind-stress and wave heights in extreme (e.g. TC) conditions, including the “ST4” source terms used in the WaveWatch III implementation used for the CAWCR hindcast (Liu et al. 2017). Despite this and other progress towards the overall excellent performance of third-generation wave models (such as WaveWatch III) to simulate TC wave fields, known shortcomings remain. Beyond the issue of TCs (sometimes) simply not being well resolved at the spatial discretizations typically used in global/regional wave models, there is a known tendency of WaveWatch III (e.g. using ST4 physics) to overestimate waves traveling in the oblique and opposing winds (as would occur in a tight-radius TC); see extensive discussion on these topics in Liu et al. (2017) and Zieger et al. (2015). Additionally, although the climate reanalysis used to provide wind input (CFSR) to the wave hindcast offers perhaps the most accurate representation of TCs among extant global reanalyses (Hodges, Cobb, and Vidale 2017), it may suffer shortcomings representing any particular TC. CFSR assimilates multiple earth observations and utilizes vortex relocation, e.g. relocating the reanalysis TC to its best-track location (Saha et al. 2013), however variations in the location and radius of the vortex and overall wind intensities may occur compared with (or due to uncertainties in) observations (Hodges, Cobb, and Vidale 2017). Both these uncertainties in the wind field, and how well the wind field is spatially resolved (CFSR has 38 km spatial resolution in the area of interest) obviously also impact the veracity of the associated simulated TC wave field.

Given these uncertainties, and since this study largely hinges on the far-field impacts of waves generated by TC Pam as represented in the CAWCR wave hindcast, the authors considered it important to perform at least a cursory verification specifically on it, rather than rely on the long-duration global/regional statistical verification provided by Durrant et al. (2014) and Hemer et al. (2016). Unfortunately, the authors are unaware of any available wave buoy observations (or other in situ wave measurements) anywhere in Kiribati, Tuvalu, Solomon Islands or Fiji during the passage of TC Pam. Therefore verified was limited to satellite altimeter estimates of H_s , in this case provided via the Ribal and Young (2019) calibrated dataset (sourced from Australia’s Integrated Marine Observing System: <http://imos.org.au/>).

The verification was performed for two different areas: the first was for the entire area indicated by Figure 1 and Figure S1a and the second was for the area indicated by Figure 2 and Figure S2b. For the first area, hourly hindcast H_s from the 0.4° resolution global grid and from the 4-arcminute (approx. 7 km) resolution nested grids surrounding Pacific islands, between March 6-17, 2015 were interpolated to a common, 4-arcminute grid (i.e. areas not

covered by the 4-arcminute nests were infilled with data from the 0.4° grid; Figure S1a indicates coverage of the 4-arcminute nests). For the second area, hourly hindcast H_s from the 4-arcminute nested grids was considered (indicated by Figure S2a. Within in both areas, hindcast H_s data was matched in space using a K-D tree search algorithm and in time by using a 30-minute window with available along-track altimeter estimates of H_s . Note that during the time period, four altimeter data platforms/bands were available: Cryosat-2, Saral, Jason-2 (C-band) and Jason-2 (KU-band); also only data >50 km from coastlines and with quality control flags indicating “*Good_data*” and “*Probably_good_data*” were used for the comparison; see Ribal and Young (2019) for more information.

Figure S1b and Figures S1c indicate scatter plots (and associated statistics) and quantile-quantile (q-q) plots respectively, for the larger area. While some scatter overall coefficients of correlation (R) and standard errors (SE) are relatively good ($R > 0.9$ and $SE < 0.004$), visual inspection of both the overall scatter and the quantiles for $H_s > \sim 9$ m noticeably diverges, e.g. the maximum matched hindcast H_s was 17.5m while altimeter H_s was 14.4 m. Figure S2b and Figures S2c indicate scatter plots and q-q plots respectively, for the smaller area and utilising only the 4-arcminute resolution nested grids, over the same time period. Here, for all but the Saral altimeter data, R is further improved (> 0.92), and the over-estimation of the hindcast H_s (relative to altimeter data) at upper quantiles is entirely absent from this smaller area more distant from Pam’s track.

The aforementioned potential shortcomings of the hindcast likely contributed to the observed differences in extreme ($\sim > 10$ m) waves between the hindcast and altimeter data near Pam’s track. Near the TC’s eye wall, where gradients in wave height are high, small errors in the location of the TC’s core in CFSR may have led to relatively large local errors in wave height; the potential for the hindcast physics to overestimate wave heights in oblique and opposing winds near the eye may have also contributed; that the TC’s track lies mostly outside of the 4-arcminute island nests and primarily within the (much coarser) 0.4° grid hindcast grid may also have contributed. Additionally, the veracity of the altimeter estimates of the extreme waves near the TC core are themselves somewhat suspect. Ribal and Young (2019) limit their calibrations of altimetric wave height to $H_s < 9.0$ m; and while this and other studies assert that altimeters accurately measure wave height up to 10 m (e.g. see also Takbash, Young, and Breivik 2019; Young, Sanina, and Babanin 2017), they are vague on verification of more extreme values, citing a lack of data. Furthermore, Timmermans et al. (2020) warns of discrepancies between altimetry products (including the Ribal and Young, 2019 dataset), particularly for extremes, raises questions about their unqualified use, and suggests “complexities specific to the estimation of extremes have to be considered, notably linked to altimeter space-time sampling of high sea states and calibration and quality control of extreme H_s values”. Attributing what portion of the apparent error between modelled versus altimetric extreme (> 10 m) wave heights is due to inadequacies of the model (i.e. in the numerical schemes, spatial resolutions, or that of the wind field used to force it), or because of inaccuracies in the various altimetric products is well beyond the scope of this paper. And in any case, it is highly doubtful sufficient observations exist in the area of study to make such a determination. This highlights the need for many more *in situ* observations of waves in the Pacific, as many other studies likewise have.

Despite these uncertainties around extreme wave heights generated near TC Pam’s vortex, as the resulting swell propagates outward, the modelled and altimetric wave heights come into better agreement, as evidenced by the high values for R and good agreement of the q-q plot shown in Figure S2; this area includes all impacted locations discussed in the main text of

this article. The authors have confidence that the CAWCR wave hindcast represented the propagation of the wave field associated with TC Pam, and its representation in the overall extreme value statistics of the hindcast, throughout the Gilbert Islands and Tuvalu reasonably well and sufficiently support the paper's conclusion.

References

- Durrant, Tom, DJM Greenslade, Mark Hemer, and Claire Trenham. 2014. "A Global Wave Hindcast Focussed on the Central and South Pacific." *CAWCR Technical Report 70*: 1–54. http://www.cawcr.gov.au/publications/technicalreports/CTR_070.pdf.
- Hemer, Mark A., Stefan Zieger, Tom Durrant, Julian O'Grady, Ron K. Hoeke, Kathleen L. McInnes, and Uwe Rosebrock. 2016. "A Revised Assessment of Australia's National Wave Energy Resource." *Renewable Energy*, 2016. <https://doi.org/10.1016/j.renene.2016.08.039>.
- Hodges, Kevin, Alison Cobb, and Pier Luigi Vidale. 2017. "How Well Are Tropical Cyclones Represented in Reanalysis Datasets?" *Journal of Climate* 30 (14): 5243–64. <https://doi.org/10.1175/JCLI-D-16-0557.1>.
- Liu, Qingxiang, Alexander Babanin, Yalin Fan, Stefan Zieger, Changlong Guan, and Il Ju Moon. 2017. "Numerical Simulations of Ocean Surface Waves under Hurricane Conditions: Assessment of Existing Model Performance." *Ocean Modelling* 118 (October): 73–93. <https://doi.org/10.1016/j.ocemod.2017.08.005>.
- Ribal, Agustinus, and Ian R. Young. 2019. "33 Years of Globally Calibrated Wave Height and Wind Speed Data Based on Altimeter Observations." *Scientific Data* 6 (1): 77. <https://doi.org/10.1038/s41597-019-0083-9>.
- Saha, Suranjana, Shrinivas Moorthi, Xingren Wu, Jiande Wang, Sudhir Nadiga, Patrick Tripp, David Behringer, et al. 2013. "The NCEP Climate Forecast System Version 2." *Journal of Climate*, September, 130925135638001. <https://doi.org/10.1175/JCLI-D-12-00823.1>.
- Takbash, Alicia, Ian R. Young, and Øyvind Breivik. 2019. "Global Wind Speed and Wave Height Extremes Derived from Long-Duration Satellite Records." *Journal of Climate* 32 (1): 109–26. <https://doi.org/10.1175/JCLI-D-18-0520.1>.
- Timmermans, B. W., C. P. Gommenginger, G. Dodet, and J.-R. Bidlot. 2020. "Global Wave Height Trends and Variability from New Multimission Satellite Altimeter Products, Reanalyses, and Wave Buoys." *Geophysical Research Letters* 47 (9). <https://doi.org/10.1029/2019GL086880>.
- Young, Ian R., E. Sanina, and A. V. Babanin. 2017. "Calibration and Cross Validation of a Global Wind and Wave Database of Altimeter, Radiometer, and Scatterometer Measurements." *Journal of Atmospheric and Oceanic Technology* 34 (6): 1285–1306. <https://doi.org/10.1175/JTECH-D-16-0145.1>.
- Zieger, Stefan, Alexander V. Babanin, W. Erick Rogers, and Ian R. Young. 2015. "Observation-Based Source Terms in the Third-Generation Wave Model WAVEWATCH." *Ocean Modelling* 96 (December): 2–25. <https://doi.org/10.1016/j.ocemod.2015.07.014>.

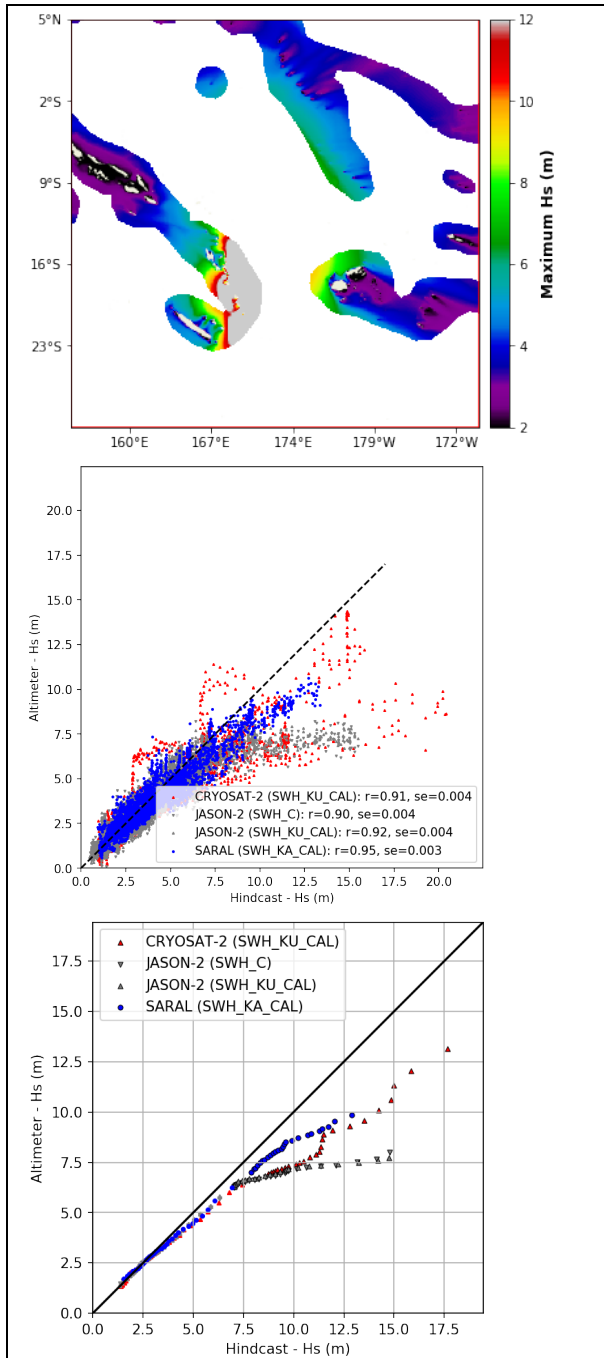


Figure S1: Satellite Altimeter/CAWCR hindcast H_s comparison, larger area, between 2015-3-5 and 2015-3-16. a): area of comparison, with colormap shading indicating the location of 4-arcminute nested grids; b) scatter plot matched altimeter/hindcast H_s , correlation (r) and standard error (se) for each altimeter included in the legend; and c) quantile-quantile plot of H_s .

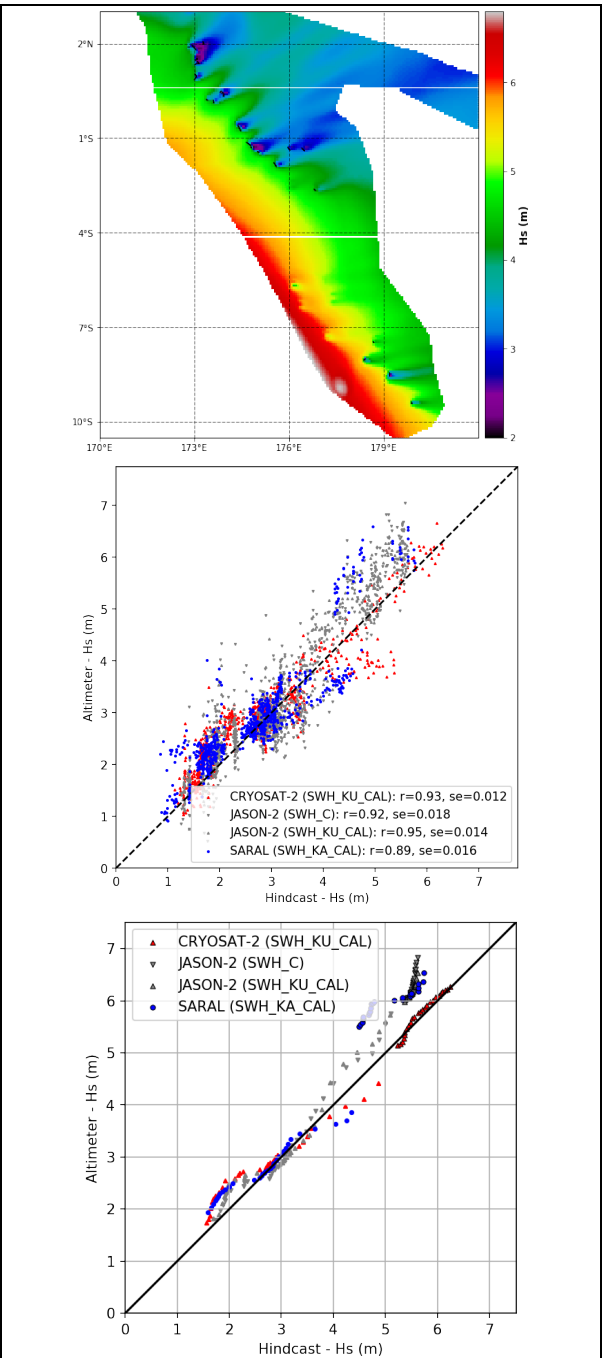
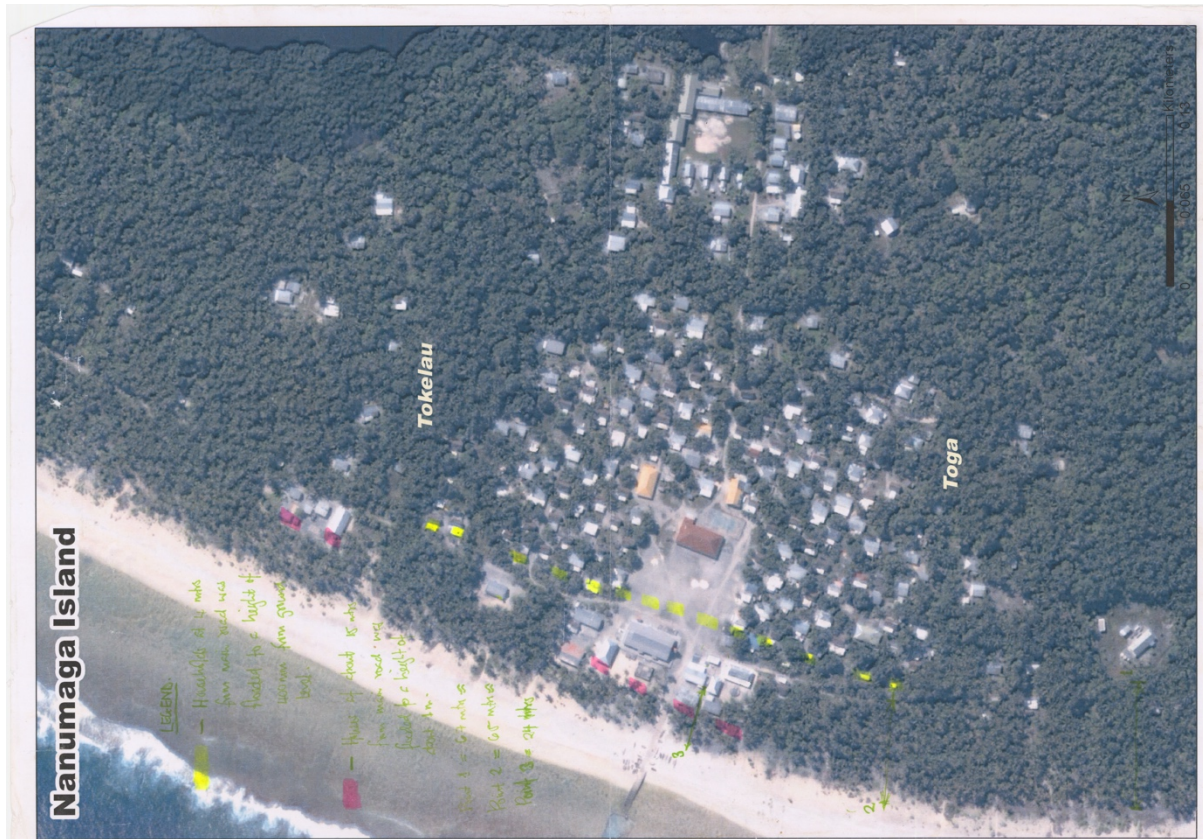


Figure S2: Satellite Altimeter/CAWCR hindcast H_s comparison, smaller area, between 2015-3-5 and 2015-3-16; a): area of comparison, with colormap shading indicating the location of 4-arcminute nested grids; b) scatter plot matched altimeter/hindcast H_s , correlation (r) and standard error (se) for each altimeter included in the legend; and c) quantile-quantile plot of H_s .

Section 2: Inundation maps provided by Tuvalu Public Works Department during post disaster survey





Niutao Island



NUKUPETAU ISLAND



NUKULAE LAE ISLAND



Oil spillage from this main corridor Building (Green Diesel) Some of it also ended up in the nearest pit

houses on W side close to beach destroyed



Western side erosion 15-20m from existing beach - east access road limited access -> inundation up to road harbour access seemed OK.